Stochastic properties of strongly coupled plasmas

I. V. Morozov*
Department of Physics, Chair of General Physics and Wave Processes, Lomonosov Moscow State University, Vorob'evy Gory, 119899, Moscow, Russia

G. E. Norman† and A. A. Valuev
Moscow Institute of Physics and Technology, Institutskii per. 9, 141700, Dolgoprudnyi, Russia
(Received 31 August 2000; published 27 February 2001)

Stochastic properties of equilibrium strongly coupled plasmas are investigated by a molecular dynamics method. The Krylov-Kolmogorov entropy K and the dynamical memory time t_m are calculated both for electrons and ions with mass ratios $10-10^5$. Two values of K entropy for ions are discovered corresponding to electron and ion time scales. The dependence of the K entropy on the number of particles, the nonideality parameter, and the form of the interaction potential is investigated. The problem of the accuracy of molecular dynamics simulations is discussed. A universal relation between Kt_m and the fluctuation of the total energy of the system is obtained. The relation does not depend on the numerical integration scheme, temperature, density, and the interparticle interaction potential, so that it may be applied to arbitrary dynamic systems. Transition from dynamic to stochastic correlation is treated for both electron and ion velocity autocorrelation functions, for Langmuir and ion-sound plasma wave dynamic structure factors. We point to quantum uncertainty as a physical reason which limits dynamic (Newton) correlation for times greater than t_m.

DOI: 10.1103/PhysRevE.63.036405 PACS number(s): 52.27.Gr, 52.65.Cc, 02.70.Ns

I. INTRODUCTION

The divergence of particle trajectories in many-body systems and the Krylov-Kolmogorov entropy (K entropy, the Lyapunov exponent) are of considerable interest in studies of the origin of irreversibility [1–12]. They were investigated using the molecular dynamics method for neutral particles [2–8,13,14] and different plasma models [12,15–17]. Another point is that the K entropy determines the rate of entropy growth in nonequilibrium processes [1,5,18], so that the K^{-1} can be considered as an important relaxation time scale.

Another quantity of interest is the predictability time τ_{pr} which was introduced in Refs. [19–22]. It determines the time interval during which the behavior of a dynamic system can be predicted from initial conditions and deterministic equations of motion. Kravtsov and co-workers [21–24] considered the measuring noise, fluctuation forces, and uncertainty about the differential deterministic equations of the system as the reasons why τ_{pr} has a finite value. The predictability horizon τ_h is defined as a limiting value of τ_{pr} when the levels of measuring noise and knowledge uncertainty are neglected. Both τ_{pr} and τ_h are proportional to λ_+^{-1}, where λ_+ is the maximum positive Lyapunov exponent. The proportionality coefficient is logarithmically dependent on the noise level. It was supposed that the system correlation time is $\tau_c=0.5\lambda_+^{-1}$ [19,21,22].

Zaslavsky [1] used the terms K entropy and the correlation uncoupling time τ_u. The K value corresponds to λ_+ averaged over the phase space, and the τ_u value corresponds to τ_h. However, it was supposed that $\tau_u=\lambda_+^{-1}$.

The dynamic memory time t_m [6,7,25] is a characteristic of a simulation model. It determines the accuracy of calculations of system properties such as time correlation functions and the dynamic structure factor in the molecular dynamics method. The times t_m, τ_{pr}, τ_h and τ_u are of close nature, and the difference between them lies only in the type of mixing noise which is taken into account. The physical meaning of the time t_m, its relation to the K entropy, and the total-energy fluctuations are studied for plasmas in the present paper.

The interparticle interaction potentials employed, and the method for studying the divergence of trajectories, are presented in Sec. II. Results for electron and ion K entropy and the dynamical memory time are given in Sec. III. Two values of K entropy for ions were found. The relation between the K entropy and the rate of entropy growth, S, is discussed in Sec. IV. A universal formula is obtained which relates the K entropy to the dynamical memory time and the total energy fluctuation. Section V is devoted to distinguishing between dynamic and stochastic correlations for both electrons and ions in strongly coupled plasmas (SCP's). The origin of the noise is related to the quantum uncertainty resulting from the weak degeneracy of electrons.

II. SIMULATION

A. Plasma model

We consider a two-component fully ionized system of $2N$ single charged particles with masses m (electrons) and M (ions). The molecular dynamics method (MDM) [2,7,8,13,26–30] was applied. Classical equations of motion are solved numerically with periodic boundary conditions.

*Email address: bogous@orc.ru
†Email address: henry_n@orc.ru

We use a ''leapfrog'' scheme of a second order approximation which, being rather simple, ensures the conservation of the average total energy [30].

It is assumed that particles of the same charge interact via a Coulomb potential, whereas the interaction between particles with different charges was described by an effective pair potential (''pseudopotential'') [31–37]. Most calculations in the present paper were performed with the electron-ion potential [32,38]

$$\Phi_{ei}(r)=\begin{cases}-e^2/r, & r>a\\ -e^2/a, & r<a,\end{cases} \tag{1}$$

where a is a cutoff length. This approximation is used in order to avoid the formation of bound states in the system. In the present simulations this parameter was taken to be $a=e^2/\varepsilon k_B T$, where T is the equilibrium temperature, k_B is the Boltzmann constant, and $\varepsilon=3$. This corresponds to the assumption that all bound states below $k_B T$ are excluded from the calculation of the Slater sum [32]. Moreover, the proportionality $a\sim T^{-1}$ yields uniformity of the interaction potential, and provides a similarity; i.e., any reduced value depends only on the nonideality parameter $\gamma=e^2 n^{-1/3}/kT$, where $n=n_e+n_i$ is the total density of charged particles.

At the first step of the simulation the system was brought to equilibrium for electrons and ions of equal masses, since the equilibrium distribution of the coordinates of particles does not depend on their masses. To obtain the required temperature of the plasma, equations of motion were solved with additional Langevin forces and friction forces proportional to velocity. In further calculations of the dynamical properties, these additional forces were dropped, and the mass ratio was restored to the correct value. At this stage we also excluded the total momentum of the particles. So that a state of the fully equilibrium isothermal plasma was achieved.

B. Calculation procedure

In order to obtain the average Lyapunov exponent, a long molecular dynamics (MD) trajectory was first computed for given plasma parameters. Then a number I of statistically independent sample phase points was chosen from this phase trajectory, and the electrons were slightly randomly displaced at these points. The system trajectories were computed using these changed electron coordinates and the former values of the electron velocities and ion phase variables as the initial conditions. After an averaging over $I=50-300$ initial configurations, the squared divergences of coordinates and velocities are calculated as

$$\langle \Delta v^2(t)\rangle=\frac{1}{NI}\sum_{j,k}^{N,I}[v_{jk}(t)-v'_{jk}(t)]^2, \tag{2}$$

$$\langle \Delta r^2(t)\rangle=\frac{1}{NI}\sum_{j,k}^{N,I}[r_{jk}(t)-r'_{jk}(t)]^2, \tag{3}$$

where $v'_{jk}(t)$ and $v_{jk}(t)$ $[r'_{jk}(t)$ and $r_{jk}(t)]$ are velocities (coordinates) of particles for new and former trajectories, respectively; $j=1,\ldots,N$ for electrons and ions, and $k=1,\ldots,I$ is the averaging index. It should be noted that real coordinates are used here rather than their images in the basic MD cell. Computations (2) and (3) were performed separately for electrons and ions.

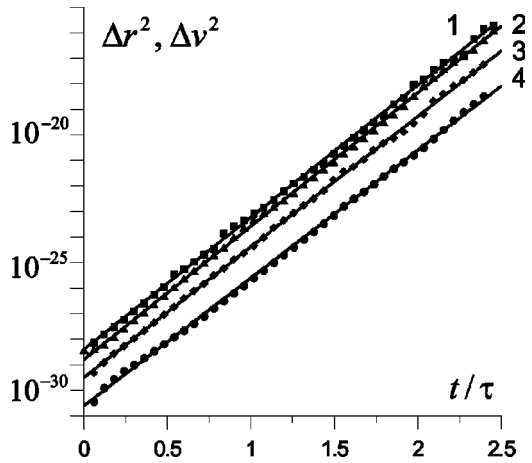

FIG. 1. Squared divergences Δv^2: (1) electrons, (3) ions; Δr^2: (2) electrons, (4) ions. $\gamma=1.5$, $M/m=10$, and $N=100$. Δr is given in Landau length units in Figs. 1–4.

Then Lyapunov exponent K can be obtained from

$$\langle \Delta v^2(t)\rangle=A\exp(Kt), \quad \langle \Delta r^2(t)\rangle=B\exp(Kt)$$

at

$$t_l<t<t_m. \tag{4}$$

Here t_l is a small time, after which the trajectory's divergence starts to follow an exponential law. On the other hand, the exponential increase of $\langle \Delta v^2(t)\rangle$ is limited by the finite value of the thermal velocity of particles. Thus, after a time t_m,

$$t>t_m\approx K^{-1}\ln(6kT/Am), \tag{5}$$

a ''saturation'' occurs [6–8], i.e.,

$$\langle \Delta v^2(t)\rangle=2\langle v^2\rangle=6kT/m, \tag{6}$$

$$\langle \Delta r^2(t)\rangle=6D(t-t_m)+\langle \Delta r^2(t_m)\rangle, \tag{7}$$

where $3kT/m$ is the thermal velocity squared, and D is the (self-) diffusion coefficient.

III. RESULTS

A. *K* entropy for electrons

Examples of $\langle \Delta v^2(t)\rangle$ and $\langle \Delta r^2(t)\rangle$ for electrons and ions is presented in Fig. 1. The values of Δv and Δr are measured in $(kT/m)^{1/2}$ and $e^2/(kT)$, respectively. The values of K turn out to be the same for both velocity and coordinate deviations. It is also seen that the K values for electrons and ions are close to each other at the initial stage of divergence. This might be related to the fact that a SCP is a system in which the fraction of collective degrees of freedom is comparable to unity [39], or to a general property of sys-

TABLE I. Dependence of $K\tau$ on the number of particles.

N	10	14	20	40	100	200
$K\tau$	11.1	12.5	11.7	11.8	12.1	12.4

tems of particles with different masses. Note that the value of K does not depend on the initial displacement (also see Ref. [15]).

B. Dependence of K entropy on the number of particles and the form of the electron-ion potential

The dependence of $K\tau$, where $\tau=2\pi/\Omega_e$ is the period of plasma oscillations, on the particle number N, is weak (Table I), which is in agreement with the results for systems of neutral particles [6,8,13]. The average errors in Table I as well as Table II are about 2%, and correspond to the interval of scattering for the electron and ion results for $\langle \Delta v^2(t)\rangle$ and $\langle \Delta r^2(t)\rangle$ [17].

The above results were obtained for the effective pair potential [Eq. (1)]. In order to show the relative contributions of the Coulomb long range interaction and the non-Coulomb short range part of the interaction to K entropy, the computations were performed for the following electron-ion potential (insertion in Fig. 2):

$$\Phi_{ei}(r)=0.1\,kT(e^2/\varepsilon kTr)^{12}-e^2/r. \tag{8}$$

Since potentials (1) and (8) satisfy the similarity relations, the value $K\tau$ depends only on the nonideality parameter γ for a given potential. The results are presented in Fig. 2 and Table II. It is seen that the form of the short range interaction does not significantly affect the K entropy in accordance with the general concepts of the role of short range interaction in SCP's [39]. The $K\tau$ values for Eqs. (1) and (8) differ by a factor 1.5. Neither of the electron-ion effective pair potentials [31,33–37] has a repulsive core, as in Eq. (8), which manifests the maximum discrepancy from Eq. (1). The high-temperature Deutsch potential [34,35] is more shallow than Eq. (1), and Rostock potentials [31,36] might have deeper minima than Eq. (1). Test calculations [40] showed that the difference of K for these is within the factor 1.8 from Eq. (1) for temperatures from 10^4 to 10^5 K. The case of pure Coulomb electron-ion interaction was treated in Ref. [12].

C. Results for ions. Mass dependence

The fact that K depends only slightly on the number of particles allows one to extend the calculations to greater ratio values M/m, taking $N=10$. The preliminary results were published in Ref. [16]. The results (Fig. 3) show that the K entropy for electrons and ions does not depend on M/m at the initial stage of divergence within the accuracy of the present calculations. In the following this value will be denoted as K_e.

TABLE II. Dependence of $K\tau$ on γ and the form of the potential.

γ	0.5	1.0	1.5
Potential Eq. (1)	18	11.9	9.8
Potential Eq. (8)	27	16.5	14.5

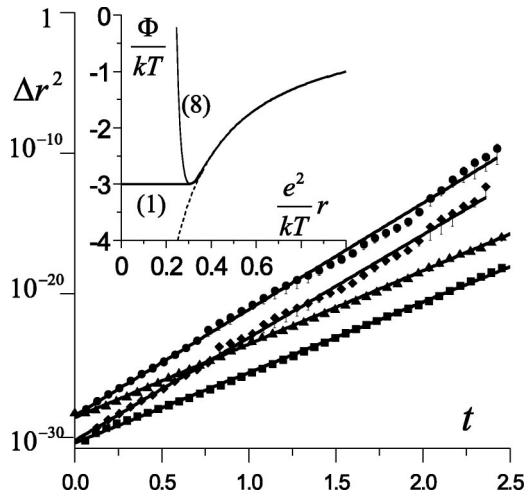

FIG. 2. Potential Eq. (1): (1) electrons, (2) ions; Eq. (8): (3) electrons, (4) ions. $\gamma=1.5$, $M/m=10$, and $N=100$.

At $t=t_m$ the quantity $\langle \Delta v^2(t)\rangle$ for electrons reaches its saturation value; therefore, at $t>t_m$, only ion trajectories continue to diverge, as seen from Fig. 4. Computations for $M/m=10-10^5$ (Figs. 4 and 5) show that there is an exponential divergence for ions with another value of K entropy depending on M/m, which will be denoted as K_i. The M/m dependence of K_e and K_i is presented in Fig. 5. Whereas the first remains constant and equal to the K_e entropy for the electrons, the second satisfy the inverse square root law $K_i \sim (M/m)^{-1/2}$

D. Dynamical memory time

Another method to obtain the Lyapunov exponent consists of calculating two trajectories with different integration time steps Δt_0 and Δt with identical initial configurations. In this case the trajectories differ at the first stage because of numerical errors. Further divergence reproduces exponential growth [Eq. (4)] with the same value of K, just as it should.

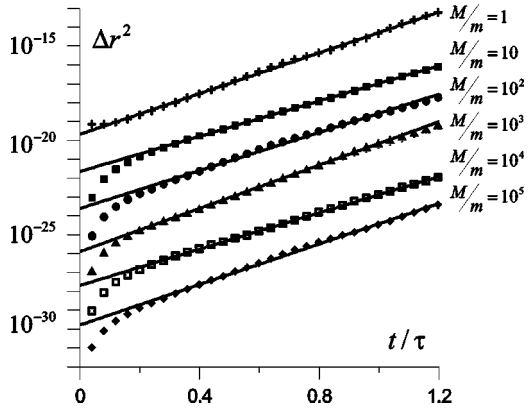

FIG. 3. Divergence Δr^2 of ions at the first time scale for different values of the mass ratio. $\gamma=1$ and $N=10$.

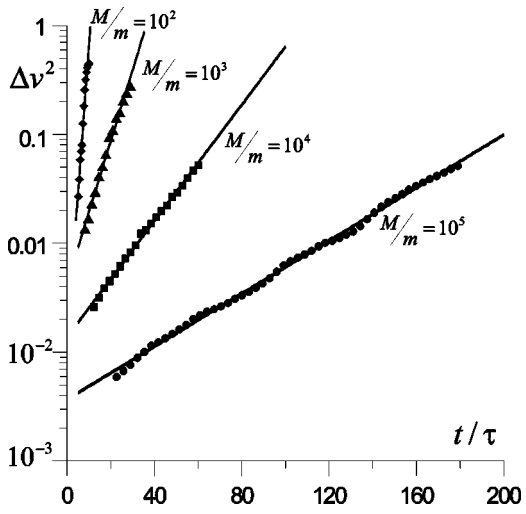

FIG. 4. Divergence Δv^2 of ions at $t>t_m$ for different mass ratios. $\gamma=1$ and $N=10$.

The values of $\langle \Delta v^2(t) \rangle$, normalized to the corresponding thermal velocities for electrons and ions, are shown in Fig. 6. The point where the exponential trend reaches the saturation level corresponds to the time t_{me}. In Fig. 6 the value of t_{me} is estimated as the moment of crossing of two straight lines. At this time the system completely ''forgets'' its initial state, and therefore t_{me} may be interpreted as a dynamical memory time. The results for t_{me}, depending on the time step ratio for the original and new trajectories, are presented in Fig. 7 as crosses. Here the integration step for the original trajectory was fixed to be equal to $\Delta t_0=0.003$ [in units $e^2m^{1/2}/(kT)^{3/2}=4.3\times10^{-15}$ s] when the step Δt for the new trajectory was varied.

The dynamical memory time can also be calculated in the following way. On the original trajectory the velocities of the particles are reversed at time points $t_1, t_2, \ldots$ (see the insert in Fig. 7). The reversed trajectory returns to the initial point

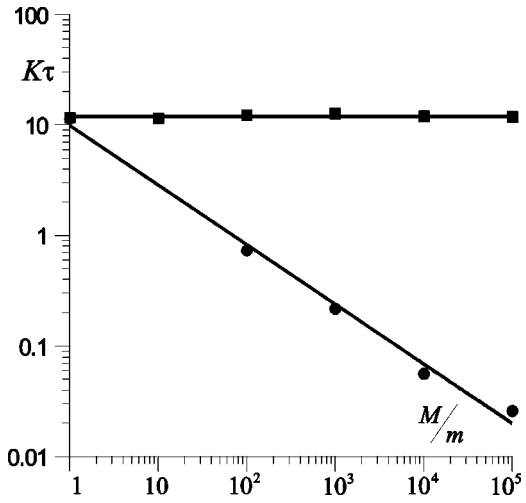

FIG. 5. Average Lyapunov exponent for ions at two time scales: squares, initial stage; circles, after saturation of electrons. In order to guide the eye, the power fits are drawn through data points. $\gamma=1$ and $N=10$.

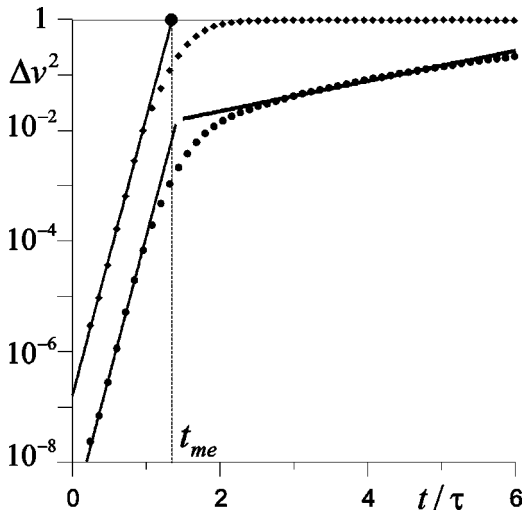

FIG. 6. The squared divergence of velocities of electrons (rhombus) and ions (circles). The lines present exponential fits corresponding to Eq. (4). $\gamma=1$, $M/m=100$, and $N=100$.

with small deviations $(\Delta r_1, \Delta v_1)$ and $(\Delta r_2, \Delta v_2)$ because of numerical errors and the Lyapunov instability. This allows us to calculate the functions $\langle \Delta r^2(2t) \rangle$ and $\langle \Delta v^2(2t) \rangle$ and obtain the dynamical memory time using a procedure analogous to that in Fig. 6. This value is shown in Fig. 7 as a triangle. One can see that it lies close to the extrapolated value of t_{me} in the limit $\Delta t \to 0$.

Figure 7 shows that the dynamical memory time for electrons depends only slightly on the step ratio $\Delta t/\Delta t_0$. Our calculations have also shown that it is true for different Δt_0. This fact can be used to plot the dependence of t_{me} on the time step for the original trajectory with any fixed value of $\Delta t/\Delta t_0$. The computation of the velocity divergence for ions after the saturation of electrons gives the value of the dynamical memory time t_{mi}. The results for both t_{me} and t_{mi} are presented in Fig. 8. The ratio t_{me}/t_{mi} is a fixed value, and

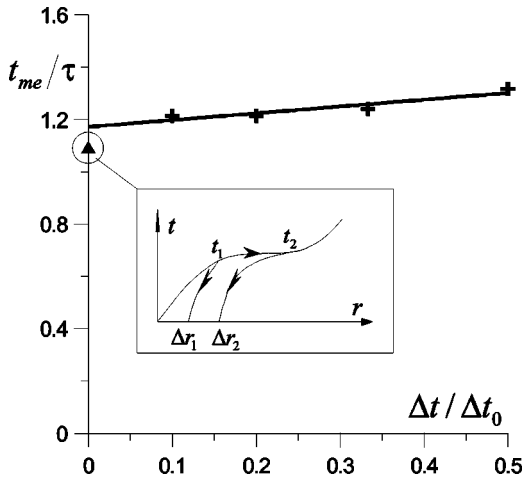

FIG. 7. The dynamical memory time for electrons depending on the trajectories time step ratio (crosses with linear fit). The triangle corresponds to the result for trajectory reversing. $\gamma=1$, $M/m=10$, and $N=100$.

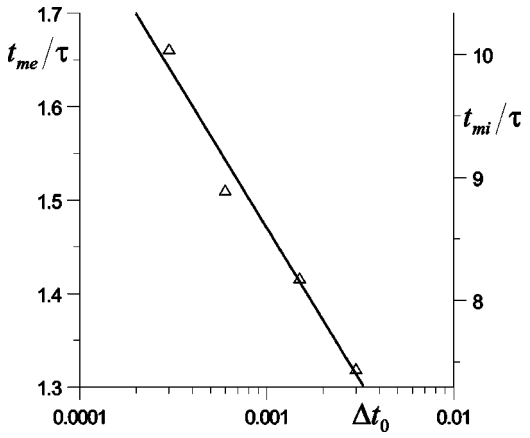

FIG. 8. The dependence of the dynamical memory time on the integration time step for electrons (t_{me}) and ions (t_{mi}). $\Delta t/\Delta t_0 = 0.5$, $\gamma = 1$, $M/m = 10$, and $N = 100$. The triangles are the results of our simulations, straight line is a logarithmic fit (its slope corresponds to $n = 2$).

does not depend on Δt_0, this so there is only one set of points in Fig. 8.

The dependence of t_{mi} on the electron-ion mass ratio is shown in Fig. 9. In accordance with the dependence of K_i (Fig. 5), it also fits the square root law.

IV. DISCUSSION

In the present paper we have calculated the K entropy and the dynamical memory time t_m for electrons and ions in SCP's. Let us now discuss how these quantities characterize stochastic properties of the system. As a preliminary issue, we start with the simplest one-component case.

A. One-component system

Physically, the value of K may be regarded as the rate of the entropy growth due to dynamic trajectory mixing.

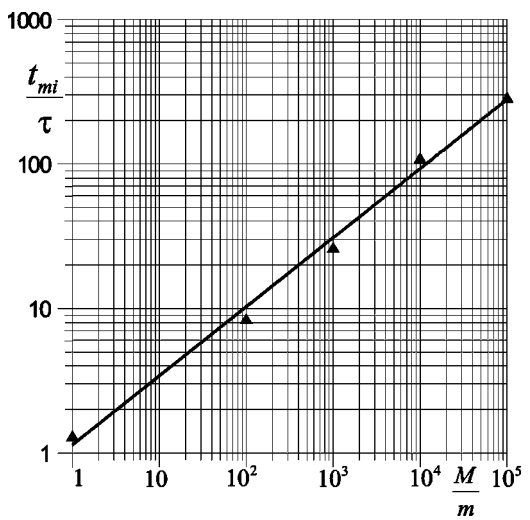

FIG. 9. The dynamical memory time for ions with different masses. The grid allows one to find t_{mi} values for definite species of ions. $\gamma = 1$ and $N = 10$.

Zaslavsky [1] considered the quantity K^{-1} as the correlation uncoupling time (see Refs. [5,18]). In order to compare these definitions with the MDM, we briefly recall arguments for this interpretation [1,5,18].

The entropy S of a subsystem in equilibrium is defined by the expression [41]

$$S = k \ln \Delta\Gamma, \tag{9}$$

where $\Delta\Gamma$ is the dimensionless statistical weight for the subsystem. Consider the motion of the phase points located initially in a compact region $\Delta\Gamma_0$ in phase space. According to Liouville's theorem, the phase volume remains constant:

$$\Delta\Gamma(t) = \Delta\Gamma_0. \tag{10}$$

Note, however, that the structure of the phase region changes drastically. Trajectories which started from initially close points inside $\Delta\Gamma_0$ diverge exponentially with time, and the structure of the region becomes more and more stretched and deformed; it is cut up, with fiords and may be fractal [5]. As a result, the effective size of the region, $\overline{\Delta\Gamma(t)}$, increases with time. From Eq. (4) it follows that

$$\overline{\Delta\Gamma(t)} = \Delta\Gamma_0 e^{ht}, \tag{11}$$

when we use a formula like $\overline{\Delta\Gamma(t)} \sim r^3 v^3$, and h is proportional to the K entropy. One can conclude from Eqs. (9) and (11) that $h \sim K$ is really a rate of entropy S growth resulting from dynamic trajectory mixing [1,5,18].

Our calculations show that the value of t_m may be treated as a time interval which is necessary for the volume $\overline{\Delta\Gamma(t)}$ to reach its maximum value $\overline{\Delta\Gamma_{max}}$. One should consider $\overline{\Delta\Gamma_{max}}$ as its value at the end of the exponential growth. During each subsequent t_m interval the procedure of filling the volume $\overline{\Delta\Gamma_{max}}$ repeats again and again without changing its value. The value of $\overline{\Delta\Gamma_{max}}$ determines the entropy of the state which is described by the MDM equilibrium phase trajectory.

From the above, it is clear that t_m has also the meaning of the correlation uncoupling time. Contrary to the suggestion of Zaslavsky [1], the values of t_m and K^{-1} can differ remarkably. Besides the quantitative difference, there is a principal difference between t_m and K^{-1}. While K is a characteristic of the many-particle system under consideration and does not depend on a numerical scheme, the value of t_m depends on the accuracy of integration, which realizes the coarse graining procedure in this case. This fact was not taken into account in Ref. [1].

The coarse graining parameter ϵ was introduced in Ref. [1] and was proposed to tend $\epsilon \to 0$ at the end of derivation. However it was assumed that the correlation uncoupling time does not depend on ϵ, and remains finite when $\epsilon \to 0$. The quantity ϵ is given by the numerical integration accuracy of the MDM. It is evident that $t_m \to \infty$ when $\epsilon \to 0$.

B. Two-component plasma

The previous arguments remain valid in this case too, but now it is necessary to consider four quantities. The values of

K_e and K_i are characteristics of the system, and do not depend on the numerical integration accuracy. K_e presents the rate of entropy growth due to the electron and ion trajectory divergence at the initial stage, and K_i defines the rate of the slower entropy growth at the stage when the electron trajectory divergence is finished but the ion trajectory divergence continues. We emphasize, once more that at the initial stage both the electron trajectory and ion trajectory divergences proceed with the same rate K_e.

The times t_{me} and t_{mi} are characteristics of the numerical scheme. These values correspond to uncoupling of electron correlation and uncoupling of ion correlation. They give the time intervals required for phase volumes $\Delta\Gamma_e$ and $\Delta\Gamma_i$ (and entropy) to reach their maximum values.

C. Universal relations

The multiplier $A\sim(\Delta t)^n$ in Eq. (4), where n is an order of approximation of the numerical integration scheme ($n=2$ for our case). Then from formula (5) one obtains

$$6kT/m = A\exp(Kt_m), \tag{12}$$

$$K(t_{m1}-t_{m2}) = n\ln(\Delta t_2/\Delta t_1), \tag{13}$$

where t_{m1} and t_{m2} are the dynamical memory times for the steps Δt_1 and Δt_2, respectively. Expression (13) does not depend on the temperature, the number density, or the system studied. K does not depend on the time step, and it allows us to illustrate $t_m(\Delta t_0)$ [Eq. (13)] in the form of Fig. 8. The slope of straight line in Fig. 8 corresponds to the logarithmic fit with $n=2$, in accordance with the numerical scheme used.

The total energy E is equal to the sum of potential and kinetic energies. The constancy of the energy E is fulfilled in MD simulations only on average. Instant values of E fluctuate around an average value. So the MD trajectory does not lie on the hypersurface $E=\text{const}$, as for Newton or Hamilton equations. It is located in a certain hyperlayer of thickness $\Delta E>0$ which envelopes the hypersurface $E=\text{const}$ [8]. The value of ΔE is determined by the accuracy of the scheme of numerical integration [6–8,30,42–44]. Since $\langle\Delta E^2\rangle\sim\Delta t^n$, it follows from Eq. (13) that

$$K(t_{m1}-t_{m2}) = \ln(\langle\Delta E_2^2\rangle/\langle\Delta E_1^2\rangle). \tag{14}$$

The form of this equation does not depend on the numerical scheme. The results for a plasma and the Lennard-Jones system [45] are presented in Fig. 10. Formula (14) relates the K entropy and the dynamical memory time to the noise level in a dynamical system and is consistent with general concepts [19,21,22]. It would appear reasonable that Eq. (14) would be a universal relation, i.e., be applicable not only to the MD systems which are used in computer simulations but to any real dynamical systems affected by noise as well.

D. General requirements to a numerical scheme

From the above discussion it follows that the time step for numerical integration must satisfy the inequalities

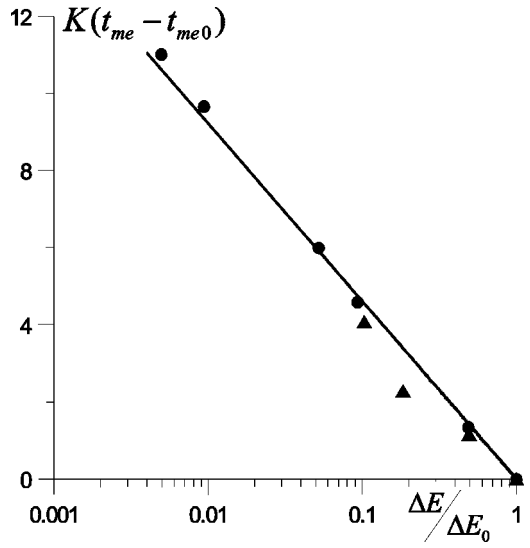

FIG. 10. The universal dependence of Kt_m on the total energy fluctuations. Triangles, SCP ($\Delta t/\Delta t_0=0.5$, $\gamma=1$, $M/m=10$, and $N=100$). Circles, Lennard-Jones system. Straight line, Eq. (14).

$$\tau_r < t_m < t_R/M, \tag{15}$$

where τ_r is a relaxation time for the process under study, t_R is the run duration, and $M^{-1/2}$ is an accuracy needed. The left inequality in Eq. (15) is evident. The right inequality reflects the fact that the points on the phase MD trajectory separated by the time interval t_m must be statistically independent. Therefore, the real accuracy of averaging is expected to be even better than $M^{-1/2}$.

Condition (15) can be naturally generalized to two-component equilibrium plasmas. In this case the values of t_R and the integration accuracy must satisfy

$$\tau_{ri} < t_{mi} < t_R/M, \tag{16}$$

where τ_{ri} is the ion relaxation time. It is expected that the averaging accuracy for electron characteristics is better than $M^{-1/2}$.

When only electron characteristics are studied, it is sufficient to take

$$\tau_{re}\sim t_R. \tag{17}$$

In this case each characteristic must be averaged over the initial ion configurations. The number of these configurations M determines the accuracy $M^{-1/2}$. Sampling procedures for the initial ion configuration differ in equilibrium and nonequilibrium cases. The definition of ensemble of initial configurations for the nonequilibrium case is a separate problem [46–48].

V. ORIGIN AND IMPORTANCE OF THE DYNAMICAL MEMORY TIME

Compare the values of the dynamical memory time obtained with the time scales of electron-ion correlation, the study of which was started for equilibrium SCP's in Refs.

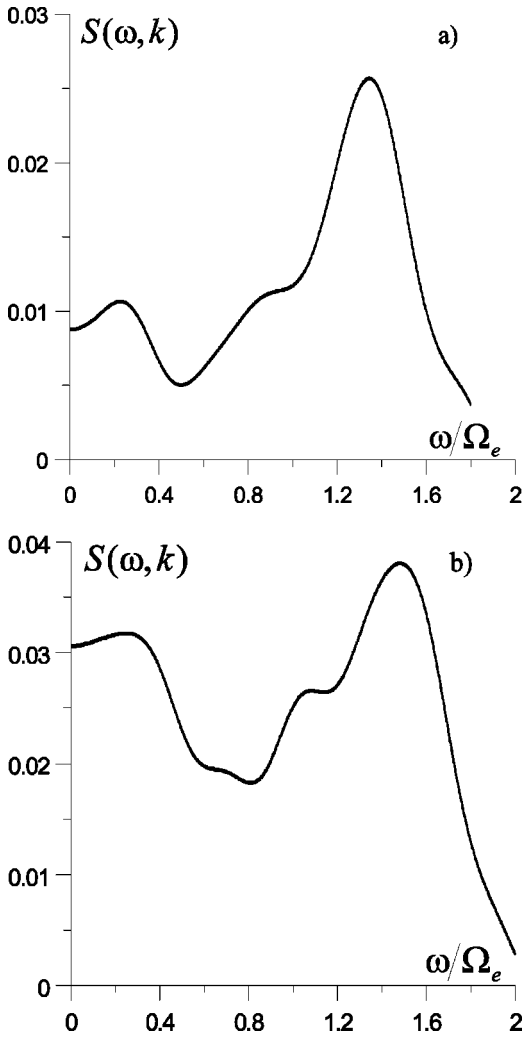

FIG. 11. The dynamical structure factors for wave numbers equal to (a) $ka_e=0.958$ and (b) $ka_e=0.857$. The first maximum corresponds to ion-sound waves, and the second to Langmuir waves. $\gamma=1$, $M/m=10$, and $N=100$.

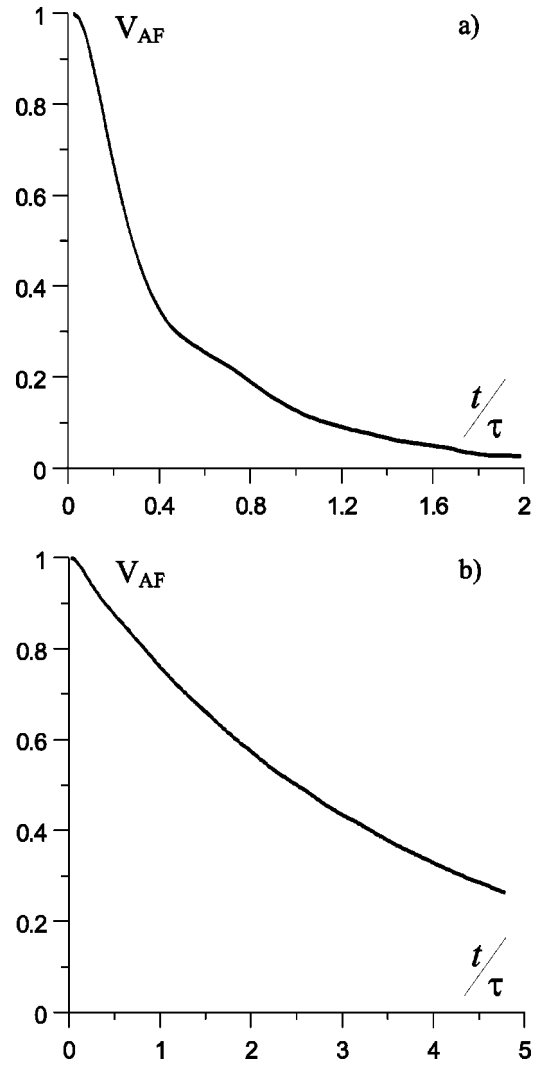

FIG. 12. Normalized velocity autocorrelation functions for (a) electrons and (b) ions. $\gamma=1$, $M/m=10$, and $N=100$.

[26,37,38,49]. The examples of our results for the dynamical structure factor (DSF) and velocity autocorrelation functions (V_{AF}) are presented in Figs. 11 and 12.

A. Electron correlation

The frequencies in the region of the electron DSF maximum and to the right correspond to times $t<t_{me}$. The same is valid for V_{AF} in the time interval when V_{AF} is greater than 0.1. Therefore, these correlations are of a dynamical (Newtonian) nature. The electron correlations for the V_{AF} tail, in the region of the DSF minimum, and to the left, correspond to the time interval when the dynamical memory of initial conditions is lost, i.e., the correlations have not a dynamic but a stochastic nature.

It would be of interest to investigate whether the increase of the dynamical memory time with improving numerical integration accuracy would influence correlation character in a range intermediate between dynamical and stochastic correlations. From a computational point of view this problem is not a simple one. It is seen from Eqs. (13) and (14) and Figs. 8 and 10 that the value of t_{me} increases only logarithmically with an improvement of the accuracy. The computational facilities available allow one to decrease ΔE by five orders of magnitude even when refined numerical schemes are used [42–44]. It would increase t_{me} only twice. Therefore the range of stochastic correlations would still be retained.

At the same time the excessive increase of t_{me} is of no importance for physics. Recall that there are natural factors which result in finite the dynamical memory time in real systems [9,10,21,22]. These include a broadening of the particle wave packets, and diffraction effects at scattering. These factors were taken into account in Refs. [10,50] to introduce a concept of quasiclassical trajectories, and to obtain the corresponding equations of motion; i.e., when passing to the classical limit the leading terms in the Plank constant power expansion are retained. The equations obtained differ from Newtonian ones by additional random forces. Gertsenshtein and Kravtsov [24] paid attention to the role of weak inelastic processes. They considered perturbations of trajectories under the influence of a thermal electromagnetic

field [19] and spontaneous radiation of low-frequency photons [23]. The fitting of the numerical integration errors to the value of the quantum noise will be studied elsewhere.

However, even now one can say that for the plasma investigated the quantum effects mentioned above are not negligible; in addition, the degeneration the degeneration parameter is not too small [26]. Taking into account that t_{me} depends on the noise level only logarithmically, it is believed that quantum uncertainty would lead to values of t_{me} which are of the same order as those obtained in this paper. Emphasize that here we discuss the dynamical memory time for real SCP's rather than for the computer model.

Thus the electron time correlations for SCP's can be of both dynamical and stochastic natures, depending on the time interval studied considered. The possible slight differences in the electron-ion effective interaction potentials discussed in Sec. III B do not violate this conclusion.

B. Ion correlation

As seen from Figs. 11 and 12(b), and from the discussion in Sec. V A, ion correlations correspond to the time when electron correlations are stochastic, the stochastization occurring many times. This is the case in both computer plasmas and real SCP's.

As for the time scale for ion V_{AF} and ion sound, the situation is quite analogous to that for electrons. These correlations are of dynamical character except in the long wavelength region of DSF's and long tail of ion V_{AF} where the correlations become stochastic. Despite the fact that the ion mass is much greater than the electron mass, the ion stochastization in real plasmas, as for electrons, is related to the quantum uncertainty. The latter is the sum of the ion uncertainty and the uncertainty induced by the electron-ion interaction. The total uncertainty level for ions is expected to be much less than for electrons. However, the ion correlation time scale is much greater than the electron time scale, and it is sufficient for the exponential instability to bring the small quantum uncertainty to a stochastic level for the ion DSF long wavelength and the V_{AF} tail.

VI. CONCLUSION

In this paper calculations of the dynamic memory time were performed for the specific case of MDM numerical schemes. Hence the values of t_{me} and t_{mi} were determined by the noise resulting from numerical errors. However, the fact that the dependence of the dynamical memory time upon the noise level is logarithmic, i.e., quite weak, allows one to extend the qualitative conclusions to the real SCP where finite values of dynamical memory time are determined by the quantum uncertainty. Therefore, the correlations for SCP's, become stochastic for long wavelength regions of both Langmuir and ion-sound plasma, waves and for long electron and ion V_{AF} tails. The specific values of the times of transition from dynamical to stochastic correlations depending on quantum effects will be considered elsewhere.

Note added in proof. The stochastic properties of one-component plasma were analyzed using the close approach described in Refs. [51–53].

ACKNOWLEDGMENTS

The authors are thankful to W. Ebeling, Yu. A. Kravtsov, V. G. Morozov, and V. V. Stegailov for valuable discussions and useful comments. The work was supported by the RFBS (Grant No. 00-02-16310).

[1] G. M. Zaslavsky, *Stochastisity of Dynamic Systems* (Nauka, Moscow, 1984) (in Russian).
[2] W. G. Hoover, *Computational Statistical Mechanics* (Elsevier, Amsterdam, 1991).
[3] W.G. Hoover and H.A. Posch, Phys. Rev. E **49**, 1913 (1994).
[4] W.G. Hoover and H.A. Posch, Phys. Rev. A **38**, 473 (1998).
[5] W. G. Hoover, *Time Reversibility, Computer Simulation and Chaos* (World Scientific, Singapore, 1999).
[6] G. E. Norman, V. Yu. Podlipchuk and A. A. Valuev, in *Termodinamika neobratimykh processov*, edited by A. I. Lopushanskaya (Nauka, Moscow, 1987), p. 11 (in Russian).
[7] A. A. Valuev, G. E. Norman, and V. Yu. Podlipchuk, in *Mathematical Modelling*, edited by A. A. Samarskii and N. N. Kalitkin (Nauka, Moscow, 1989), p. 5 (in Russian).
[8] G.E. Norman, V.Yu. Podlipchuk, and A.A. Valuev, J. Mosc. Phys. Soc. **2**, 7 (1992).
[9] A.S. Kaklyugin and G.E. Norman, J. Mosc. Phys. Soc. **8**, 283 (1998).
[10] A.S. Kaklyugin and G.E. Norman, Zh. Ross. Khem. Ob-va im. D.I. Mendeleeva **44** (3), 7 (2000) (in Russian).
[11] D. Zubarev, V. Morozov, and G. Roepke, *Statistical Mechanics of Nonequilibrium Processes* (Akadeimie-Verlag, Berlin, 1996).
[12] S.A. Maiorov, Kratkie Soobshchenia Fiz. FIAN No. 1, 33 (1999) Bull. Lebedev Phys. Inst. No. 1, 33 (1999)].
[13] G.E. Norman, V.Yu. Podlipchuk, and A.A. Valuev, Matematicheskoe Modelirovanie **2**, 3 (1990) (in Russian).
[14] K.-H. Kwon and B.-Y. Park, J. Chem. Phys. **107**, 5171 (1997).
[15] I.V. Morozov, G.E. Norman, and A.A. Valuev, J. Tech. Phys. **40**, 61 (1999).
[16] I.V. Morozov, G.E. Norman, and A.A. Valuev, Contrib. Plasma Phys. **39**, 307 (1999).
[17] I.V. Morozov, G.E. Norman, and A.A. Valuev, J. Phys. (France) **10**, 251 (2000).
[18] Yu. L. Klimontovich, *Statistical Theory of Open Systems* (Kluwer, Dordrecht, 1995).
[19] Yu.A. Kravtsov, Zh. Éksp. Teor. Fiz. **95**, 1661 (1989) [Sov. Phys. JETP **69**, 940 (1989)].
[20] Yu.A. Kravtsov, Usp. Fiz. Nauk **158**, 93 (1989) [Sov. Phys. Usp. **32**, 434 (1989)].
[21] Yu. A. Kravtsov, in *Limits of Predictability*, edited by Yu. A. Kravtsov (Springer, Berlin, 1993), p. 173.
[22] Yu. A. Kravtsov, in *Predely Predskazuemosti*, edited by Yu. A. Kravtsov (TsentrKom, Moscow, 1997), p. 170 (in Russian).
[23] M. E. Gertsenshtein and Yu. A. Kravtsov, Russia's Science

and technology No. 6, 9 (1998) (in Russian).
[24] M.E. Gertsenshtein and Yu.A. Kravtsov, Zh. Éksp. Teor. Fiz. **118**, 761 (2000) [JETP **91**, 658 (2000)].
[25] G. E. Norman, in *Abstracts of Reports to the Fifth All-Union Conference on the Structure and Properties of Metal and Slag Melts, 1983* (Ural Science Centre, Sverdlovsk, 1983), Vol. 1, p. 582 (in Russian).
[26] J.P. Hansen and I.R. McDonald, Phys. Rev. A **23**, 2041 (1981).
[27] *Molecular-Dynamics Simulation of Statistical Mechanical Systems* (*Proceedings of the International School of Physics ''Enrico Fermi,'' Course 97*), edited by G. Ciccotti and W. G. Hoover (North-Holland, Amsterdam, 1986).
[28] M. P. Allen and D. J. Tildesley, *Computer Simulation of Liquids* (Clarendon, Oxford, 1987).
[29] W. F. van Gunsteren, in *Mathematical Frontiers in Computational Chemical Physics*, edited by D. Truhler (Springer, New York, 1988), p. 136.
[30] G.E. Norman, V.Yu. Podlipchuk, and A.A. Valuev, Mol. Simul. **9**, 417 (1993).
[31] W. Ebeling, Ann. Phys. (Leipzig) **19**, 104 (1967); **21**, 315 (1968); **22**, 33 (1969); **22**, 383 (1969); **22**, 392 (1969).
[32] B.V. Zelener, G.E. Norman, and V.S. Filinov, Teplofiz. Vys. Temp. **10**, 1160 (1972) [High Temp. **10**, 1043 (1972)].
[33] W. Ebeling and R. Sändig, Ann. Phys. (Leipzig) **28**, 289 (1973).
[34] C. Deutsch, Phys. Lett. **60A**, 317 (1977).
[35] C. Deutsch, M.M. Gombert, and H. Minoo, Phys. Lett. **66A**, 381 (1978); **72A**, 481 (1979).
[36] W. D. Kraeft, D. Kremp, W. Ebeling, and R. Röpke, *Quantum Statistic of Charged Particle Systems* (Akademie-Verlag, Berlin, 1996).
[37] W. Ebeling, G.E. Norman, A.A. Valuev, and I.A. Valuev, Contrib. Plasma Phys. **39**, 61 (1999).
[38] I.V. Morozov, G.E. Norman, and A.A. Valuev, Dokl. Akad. Nauk. **362**, 752 (1998) [Phys. Dokl. **43**, 608 (1998)].
[39] A.A. Valuev, A.S. Kaklyugin, and G.E. Norman, Zh. Éksp. Teor. Phys. **113**, 880 (1998) [JETP **86**, 480 (1998)].
[40] W. Ebeling and I. V. Morozov (unpublished).
[41] L. D. Landau, E. M. Lifshiz, *Statistical Physics* (Nauka, Moscow, 1995) (in Russian).
[42] G.J. Rowlands, Comput. Phys. **97**, 235 (1991).
[43] M.A. Lopez-Marcos, J.M. Sanz-Serna, and J.C. Diaz, J. Comput. Appl. Math. **67**, 173 (1996).
[44] M.A. Lopez-Marcos, J.M. Sanz-Serna, and R.D. Skeel, SIAM (Soc. Ind. Appl. Math.) J. Sci. Stat. Comput. **18**, 223 (1997).
[45] G. E. Norman and V. V. Stegailov, Zh. Eksp. Teor. Fiz. (to be published).
[46] J.P. Hansen and I.R. McDonald, Phys. Lett. **97A**, 42 (1983).
[47] G. E. Norman and A. A. Valuev, in *Strongly Coupled Coulomb Systems*, edited by G. Kalman, M. Rommel, and K. Blagoev (Plenum Press, New York, 1998), p. 103.
[48] G.E. Norman, A.A. Valuev, and I.A. Valuev, J. Phys. (France) **10**, 255 (2000).
[49] J.P. Hansen and L. Sjogren, Phys. Fluids **25**, 617 (1982).
[50] A.S. Kaklyugin and G.E. Norman, J. Mosc. Phys. Soc. **5**, 223 (1995).
[51] Y/ Ueshima, K. Nishihara, D.M. Barnett, T. Tajima, and H. Furukawa, Phys. Rev. E **55**, 3439 (1997).
[52] Y. Ueshima, K. Nishihara, D.M. Barnett, T. Tajima, and H. Furukawa, Phys. Rev. Lett. **79**, 2249 (1997).
[53] D.M. Barnett, T. Tajima, and Y. Ueshima, Phys. Rev. Lett. **83**, 2677 (1999).